The Twenty-Second International Symposium on Artificial Life and Robotics 2017 (AROB 22nd 2017),
The Second International Symposium on BioComplexity 2017 (ISBC 2nd 2017),
B-Con Plaza, Beppu, Japan, January 19-21, 2017

Verification of Humanoid Robot Model Considering Stick/Slip Friction

Daiji Izawa[1], Xiang Li[1], Takayuki Matsuno[1], Mamoru Minami[1] and Akira Yanou[2]

[1]Okayama University, Japan
[2]Kawasaki College of Allied Health Professions , Japan
(Tel:81-86-251-8233, Fax:81-86-251-8233)
[1]p1k85fm3@s.okayama-u.ac.jp

Abstract: Biped locomotion created by referring to ZMP criterion to keep a robot stable during walking have contributed to promising humanoid's walking strategies, having realized stable walking of real humanoid robots. However the walking strategies having been proposed so far including ZMP-based stabilization method seem to be constructed on assumption that the slippage doesn't occur. In this paper, a walking model of humanoid robot including slipping, bumping, surface-contacting and point-contacting of foot is discussed, and its dynamical equation is derived by Newton-Euler method. And we introduce a new model that includes the slipping of supporting or lifting foot. In this thesis, we verify whether our humanoid robot model and gait models considering stick/slip friction motion are correct or not from the view point that the law of mechanical energy conservation are always kept when no energy consumption is given as a condition of motion.

Keywords: Humanoid, siliping, Bipedal, Dynamical, Newton-Euler Method

1 INTRODUCTION

Human beings have acquired an ability of stable bipedal walking in evolving repetitions so far. From a view point of making a stable controller for the bipedal walking based on knowledge of conventional control theory, it looks not easy because of the dynamics with high nonlinearity and coupled interactions between links of humanoid with high dimensions. Therefore how to simplify the complicated walking dynamics to help construct stable walking controller has been studied intensively.

Avoiding complications in dealing directly with true dynamics without approximation, an inverted pendulum model has been used frequently for making a stable controller[1]-[3], simplifying the calculations to determine input torque. Further, linear approximation having the humanoid represented by simple inverted pendulum enables researchers to realize stable gait through well-known control strategy[4]-[6].

Our research has begun from the view point as aiming to describe gait's dynamics as correctly as possible, including point-contacting state of foot and toe, slipping of the foot and bumping [7] [8]. The dynamics of humanoid is discussed not only leg but also head, waist and arms. And that what we think more important is that the dimension of dynamical equation changes depending on the walking gait's varieties, which has been discussed by [9] about concerning one legged hopping robot. But in this reference, walking exercise isn't mentioned. And there is no report that the dimension number of state variables varies according to the result of its dynamical transitions. Further the falling down motion has been called as non-holonomic dynamics that includes a joint without inputting torque, i.e., free joint.

Meanwhile, landing of the heel or the toe of lifting leg in the air to the ground makes a geometrical contact. Based on [10]. The dynamics of humanoid can be modeled as a serial-link manipulator including constraint motion and slipping motion by using the Extended Newton-Euler(NE) Method[11].

In this research that based on [12], a walking model of humanoid robot including slipping, bumping, surface contacting and point-contacting of foot was discussed, and its dynamical equation is derived by the NE method.

In this paper, the slipping of the foot of humanoid robot when the friction coefficient is small (on the ice, snow, or wet road) has been modeled to discuss walking motion and slipping behavior. The new model of humanoid robot and gait models have been proposed. Also we confirmed that the dynamical model describe correctly the multi-body humanoid dynamics from several view points of energy consumption with/without discharging by frictions and so on. And gait models include both slip and stick will be verified through the simulation experiments.

2 DYNAMICAL WALKING MODEL BY NEWTON-EULER METHOD

2.1 Forward Kinematical Calculations

We discuss a bipedal robot whose definition is depicted in Fig.1. Table 1 lists length l_i [m], mass m_i [kg] of links and coefficient of joints' viscous friction d_i [N·m·s/rad], which are decided based on [13]. This model is simulated as a serial-link manipulator having ramifications and represents

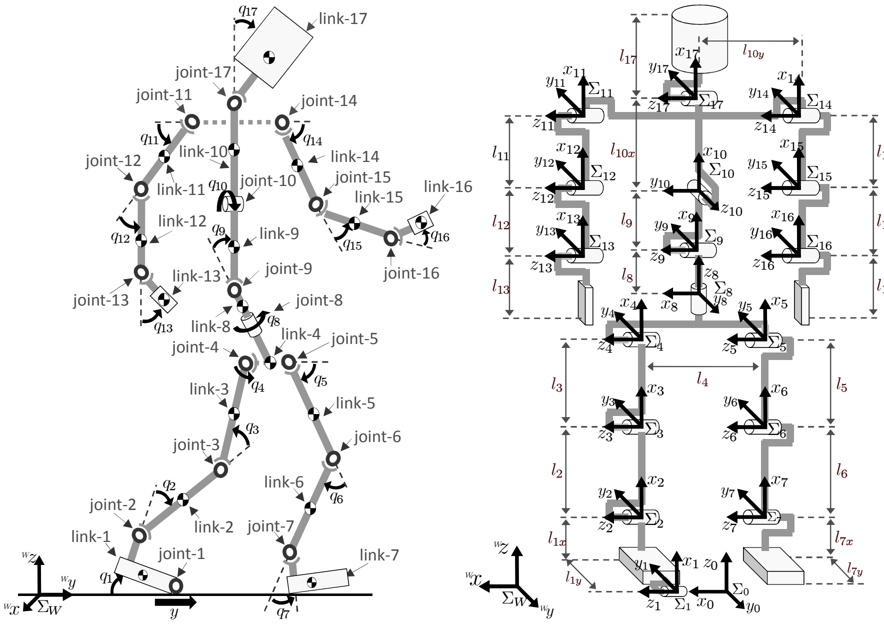

Fig. 1. Definition of humanoid's link, joint and coordinate system

Table 1. Physical parameters

Link	l_i	m_i	d_i
Head	0.24	4.5	0.5
Upper body	0.41	21.5	10.0
Middle body	0.1	2.0	10.0
Lower body	0.1	2.0	10.0
Upper arm	0.31	2.3	0.03
Lower arm	0.24	1.4	1.0
Hand	0.18	0.4	2.0
Waist	0.27	2.0	10.0
Upper leg	0.38	7.3	10.0
Lower leg	0.40	3.4	10.0
Foot	0.07	1.3	10.0
Total weight [kg]	—	64.2	—
Total hight [m]	1.7	—	—

rigid whole body—feet including toe, torso, arms and so on—by 17 DoF. Though motion of legs is restricted in sagittal plane, it generates varieties of walking gait sequences since the robot has flat-sole feet and kicking torque on ankle. In this paper, one foot including link-1 is defined as "supporting-leg" and another foot including link-7 is defined as "free-leg" ("contacting-leg" when the free-leg contacts with floor) according to the walking state.

In this paper, we derive the equation of motion following by NE formulation. So we consider the structure of the supporting leg with two situations. When the supporting leg is constituted of rotating joint, we first have to calculate relations of positions, velocities and accelerations between links as forward kinetics procedures from bottom link to top link. Serial link's angular velocity ${}^i\boldsymbol{\omega}_i$, angular acceleration ${}^i\dot{\boldsymbol{\omega}}_i$, acceleration of the origin ${}^i\ddot{\boldsymbol{p}}_i$ and acceleration of the center of mass ${}^i\ddot{\boldsymbol{s}}_i$ based on Σ_i fixed at i-th link are obtained as follows.

$$
\begin{aligned}
{}^i\boldsymbol{\omega}_i &= {}^{i-1}\boldsymbol{R}_i^T\, {}^{i-1}\boldsymbol{\omega}_{i-1} + \boldsymbol{e}_{z_i}\dot{q}_i && (1)\\
{}^i\dot{\boldsymbol{\omega}}_i &= {}^{i-1}\boldsymbol{R}_i^T\, {}^{i-1}\dot{\boldsymbol{\omega}}_{i-1} + \boldsymbol{e}_z\ddot{q}_i + {}^i\boldsymbol{\omega}_i \times (\boldsymbol{e}_{z_i}\dot{q}_i) && (2)\\
{}^i\ddot{\boldsymbol{p}}_i &= {}^{i-1}\boldsymbol{R}_i^T \Big\{ {}^{i-1}\ddot{\boldsymbol{p}}_{i-1} + {}^{i-1}\dot{\boldsymbol{\omega}}_{i-1} \times {}^{i-1}\hat{\boldsymbol{p}}_i \\
&\qquad + {}^{i-1}\boldsymbol{\omega}_{i-1} \times ({}^{i-1}\boldsymbol{\omega}_{i-1} \times {}^{i-1}\hat{\boldsymbol{p}}_i) \Big\} && (3)\\
{}^i\ddot{\boldsymbol{s}}_i &= {}^i\ddot{\boldsymbol{p}}_i + {}^i\dot{\boldsymbol{\omega}}_i \times {}^i\hat{\boldsymbol{s}}_i + {}^i\boldsymbol{\omega}_i \times ({}^i\boldsymbol{\omega}_i \times {}^i\hat{\boldsymbol{s}}_i) && (4)
\end{aligned}
$$

Then if the supporting leg is constituted of prismatic form object, that describes slipping motion along ${}^w y$ direction in Fig.1. The equations is switched as the following.

$$
\begin{aligned}
{}^i\boldsymbol{\omega}_i &= {}^{i-1}\boldsymbol{R}_i^{\mathrm{T}}\, {}^{i-1}\boldsymbol{\omega}_{i-1} && (5)\\
{}^i\dot{\boldsymbol{\omega}}_i &= {}^{i-1}\boldsymbol{R}_i^{\mathrm{T}}\, {}^{i-1}\dot{\boldsymbol{\omega}}_{i-1} && (6)\\
{}^i\ddot{\boldsymbol{p}}_i &= {}^{i-1}\boldsymbol{R}_i^{\mathrm{T}} \Big\{ {}^{i-1}\ddot{\boldsymbol{p}}_{i-1} + {}^{i-1}\dot{\boldsymbol{\omega}}_{i-1} \times {}^{i-1}\hat{\boldsymbol{p}}_i \\
&\qquad + {}^{i-1}\boldsymbol{\omega}_{i-1} \times ({}^{i-1}\boldsymbol{\omega}_{i-1} \times {}^{i-1}\hat{\boldsymbol{p}}_i) \Big\} \\
&\qquad + 2({}^{i-1}\boldsymbol{R}_i^{T\, i-1}\boldsymbol{\omega}_{i-1}) \times (\boldsymbol{e}_z\dot{q}_i) + \boldsymbol{e}_z\ddot{q}_i && (7)\\
{}^i\ddot{\boldsymbol{s}}_i &= {}^i\ddot{\boldsymbol{p}}_i + {}^i\dot{\boldsymbol{\omega}}_i \times {}^i\hat{\boldsymbol{s}}_i + {}^i\boldsymbol{\omega}_i \times ({}^i\boldsymbol{\omega}_i \times {}^i\hat{\boldsymbol{s}}_i) && (8)
\end{aligned}
$$

Here, ${}^{i-1}\boldsymbol{R}_i$ means orientation matrix, ${}^{i-1}\hat{\boldsymbol{p}}_i$ represents position vector from the origin of $(i-1)$-th link to the one of i-th, ${}^i\hat{\boldsymbol{s}}_i$ is defined as gravity center position of i-th link and $\boldsymbol{e}_{z_i}$ is unit vector that shows rotational axis of i-th link.

2.2 Backward Inverse Dynamical Calculations

After the above forward kinetic has been calculated, contrarily inverse dynamical calculation from top to base link are calculated as follow. Newton equation and Euler equation of i-th link are represented by Eqs.(9) and (10) where ${}^i\boldsymbol{I}_i$ is defined as inertia tensor of i-th link. Here, ${}^i\boldsymbol{f}_i$ and ${}^i\boldsymbol{n}_i$ in Σ_i show the force and moment exerted on i-th link from i+1-th link.

$$
\begin{aligned}
{}^i\boldsymbol{f}_i &= {}^i\boldsymbol{R}_{i+1}{}^{i+1}\boldsymbol{f}_{i+1} + m_i{}^i\ddot{\boldsymbol{s}}_i && (9)\\
{}^i\boldsymbol{n}_i &= {}^i\boldsymbol{R}_{i+1}{}^{i+1}\boldsymbol{f}_{i+1} + {}^i\boldsymbol{I}_i{}^i\dot{\boldsymbol{\omega}}_i + {}^i\boldsymbol{\omega}_i \times ({}^i\boldsymbol{I}_i{}^i\boldsymbol{\omega}_i) \\
&\qquad + {}^i\hat{\boldsymbol{s}}_i \times (m_i{}^i\ddot{\boldsymbol{s}}_i) + {}^i\hat{\boldsymbol{p}}_{i+1} \times ({}^i\boldsymbol{R}_{i+1}{}^{i+1}\boldsymbol{f}_{i+1}) && (10)
\end{aligned}
$$

On the other hand, since force and torque on 5th and 8th links are exerted on 4th link, effects onto 4th link as:

$$
\begin{aligned}
{}^4\boldsymbol{f}_4 &= {}^4\boldsymbol{R}_5{}^5\boldsymbol{f}_5 + {}^4\boldsymbol{R}_8{}^8\boldsymbol{f}_8 + m_4{}^4\ddot{\boldsymbol{s}}_4, &(11)\\
{}^4\boldsymbol{n}_4 &= {}^4\boldsymbol{R}_5{}^5\boldsymbol{n}_5 + {}^4\boldsymbol{R}_8{}^8\boldsymbol{n}_8 + {}^4\boldsymbol{I}_4{}^4\dot{\boldsymbol{\omega}}_4 + {}^4\boldsymbol{\omega}_4 \times ({}^4\boldsymbol{I}_4{}^4\boldsymbol{\omega}_4)\\
&\quad + {}^4\hat{\boldsymbol{s}}_4 \times (m_4{}^4\ddot{\boldsymbol{s}}_4) + {}^4\hat{\boldsymbol{p}}_5 \times ({}^4\boldsymbol{R}_5{}^5\boldsymbol{f}_5)\\
&\quad + {}^4\hat{\boldsymbol{p}}_8 \times ({}^4\boldsymbol{R}_8{}^8\boldsymbol{f}_8). &(12)
\end{aligned}
$$

Similarly, force and torque on 11th, 14th and 17th links act on 10th link directly. Then, rotational motion equation of i-th link is obtained as Eq.(13) by making inner product of induced torque onto the i-th link's unit vector $\boldsymbol{e}_{z_i}$ around rotational axis,

$$\tau_i = \boldsymbol{e}_{z_i}^T\,{}^i\boldsymbol{n}_i + d_i\dot{q}_i. \tag{13}$$

However, when the supporting leg (1st link) is slipping (prismatic joint), the force onto the 1st link can be calculated by following equation.

$$f_1 = \boldsymbol{e}_{z_1}^T\,{}^1\boldsymbol{f}_1 + \mu_k\dot{y}_0. \tag{14}$$

Finally, we get motion equation with one leg standing as:

$$\boldsymbol{M}(\boldsymbol{q})\ddot{\boldsymbol{q}} + \boldsymbol{h}(\boldsymbol{q},\dot{\boldsymbol{q}}) + \boldsymbol{g}(\boldsymbol{q}) + \boldsymbol{D}\dot{\boldsymbol{q}} = \boldsymbol{\tau}, \tag{15}$$

Here, $\boldsymbol{\tau} = [f_1, \tau_1, \tau_2, \cdots, \tau_{17}]$ is input torque, $\boldsymbol{M}(\boldsymbol{q})$ is inertia matrix, both of $\boldsymbol{h}(\boldsymbol{q},\dot{\boldsymbol{q}})$ and $\boldsymbol{g}(\boldsymbol{q})$ are vectors which indicate Coriolis force, centrifugal force and gravity. When the supporting leg is slipping, the $\boldsymbol{D} = diag[\mu_k, d_1, d_2, \cdots, d_{17}]$ is a matrix which means coefficients between foot and ground, and $\boldsymbol{q} = [y_0, q_1, q_2, \cdots, q_{17}]^T$ means the relative position between foot and ground and that of joints. The vector $\boldsymbol{q}$ changes according to the state of the supporting foot as shown in Fig. 2.

2.3 Constraint Conditions for free-leg Model

When making free-leg contact with ground, the free leg appears with the position or angle to the ground being constrained. Also, when velocity of free leg's in traveling direction becomes less than 0.01[m/s], the free leg is constrained in acceleration by the static friction. The constraints of foot's z-axis position, heel's rotation and foot's y-axis position on floating foot are defined as C_1, C_2 and C_3 respectively, these

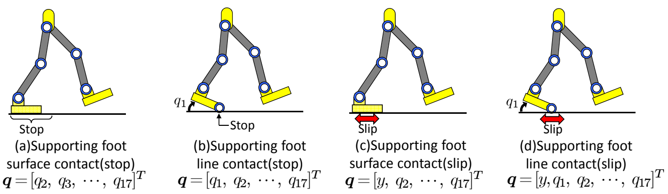

Fig. 2. Ground state of the supporting foot

constraints can be written as follow, where $\boldsymbol{r}(\boldsymbol{q})$ means heel position of free leg or toe position of it in Σ_W.

$$\boldsymbol{C}(\boldsymbol{r}(\boldsymbol{q})) = \begin{bmatrix} C_1(\boldsymbol{r}(\boldsymbol{q})) \\ C_2(\boldsymbol{r}(\boldsymbol{q})) \\ C_3(\boldsymbol{r}(\boldsymbol{q})) \end{bmatrix} = \boldsymbol{0} \tag{16}$$

Then, equation of motion with external force f_{nz}, friction force f_t, external torque τ_n and external force f_{ny} corresponding to C_1, C_2 and C_3 can be derived as:

$$
\begin{aligned}
&\boldsymbol{M}(\boldsymbol{q})\ddot{\boldsymbol{q}} + \boldsymbol{h}(\boldsymbol{q},\dot{\boldsymbol{q}}) + \boldsymbol{g}(\boldsymbol{q}) + \boldsymbol{D}\dot{\boldsymbol{q}}\\
&\qquad = \boldsymbol{\tau} + \boldsymbol{j}_{cz}^T f_{nz} - \boldsymbol{j}_t^T f_t + \boldsymbol{j}_r^T \tau_n + \boldsymbol{j}_{cy}^T f_{ny}
\end{aligned} \tag{17}
$$

where $\boldsymbol{j}_{cz}$, $\boldsymbol{j}_t$, $\boldsymbol{j}_r$ and $\boldsymbol{j}_{cy}$ are defined as:

$$
\begin{aligned}
&\boldsymbol{j}_{cz}^T = \left(\frac{\partial \boldsymbol{r}}{\partial \boldsymbol{q}^T}\right)^T \left(\frac{\partial C_1}{\partial \boldsymbol{q}^T} \Big/ \left\|\frac{\partial C_1}{\partial \boldsymbol{r}^T}\right\|\right),\ \boldsymbol{j}_t^T = \left(\frac{\partial \boldsymbol{r}}{\partial \boldsymbol{q}^T}\right)^T \frac{\dot{\boldsymbol{r}}}{\|\dot{\boldsymbol{r}}\|},\\
&\boldsymbol{j}_r^T = \frac{\partial C_2}{\partial \boldsymbol{r}^T} \Big/ \left\|\frac{\partial C_2}{\partial \boldsymbol{r}^T}\right\|,\ \boldsymbol{j}_{cy}^T = \left(\frac{\partial \boldsymbol{r}}{\partial \boldsymbol{q}^T}\right)^T \left(\frac{\partial C_3}{\partial \boldsymbol{q}^T} \Big/ \left\|\frac{\partial C_3}{\partial \boldsymbol{q}^T}\right\|\right)
\end{aligned} \tag{18}
$$

It is common sense that (i) f_{nz} and f_t are orthogonal, and (ii) value of f_t is decided by $f_t = Kf_{nz}$ $(0 < K \leq 1)$. The differentiating Eq.(16) in second order, we can derive the constraint condition of $\ddot{\boldsymbol{q}}$.

$$\left(\frac{\partial C_i}{\partial \boldsymbol{q}^T}\right)\ddot{\boldsymbol{q}} + \dot{\boldsymbol{q}}^T\left\{\frac{\partial}{\partial \boldsymbol{q}}\left(\frac{\partial C_i}{\partial \boldsymbol{q}^T}\right)\dot{\boldsymbol{q}}\right\} = 0 \quad (i = 1,\ 2,\ 3) \tag{19}$$

Making the $\ddot{\boldsymbol{q}}$ in Eqs.(17) and (19) be identical, we can obtain the equation of contacting motion as follow.

$$
\begin{bmatrix}
\boldsymbol{M}(\boldsymbol{q}) & -(\boldsymbol{j}_{cz}^T - \boldsymbol{j}_t^T K) & -\boldsymbol{j}_r^T & -\boldsymbol{j}_{cy}^T\\
\partial C_1/\partial \boldsymbol{q}^T & 0 & 0 & 0\\
\partial C_2/\partial \boldsymbol{q}^T & 0 & 0 & 0\\
\partial C_3/\partial \boldsymbol{q}^T & 0 & 0 & 0
\end{bmatrix}
\begin{bmatrix} \ddot{\boldsymbol{q}} \\ f_{nz} \\ \tau_n \\ f_{ny} \end{bmatrix}
= \begin{bmatrix}
\boldsymbol{\tau} - \boldsymbol{h}(\boldsymbol{q},\dot{\boldsymbol{q}}) - \boldsymbol{g}(\boldsymbol{q}) - \boldsymbol{D}\dot{\boldsymbol{q}}\\
-\dot{\boldsymbol{q}}^T\left\{\frac{\partial}{\partial \boldsymbol{q}}\left(\frac{\partial C_1}{\partial \boldsymbol{q}^T}\right)\right\}\dot{\boldsymbol{q}}\\
-\dot{\boldsymbol{q}}^T\left\{\frac{\partial}{\partial \boldsymbol{q}}\left(\frac{\partial C_2}{\partial \boldsymbol{q}^T}\right)\right\}\dot{\boldsymbol{q}}\\
-\dot{\boldsymbol{q}}^T\left\{\frac{\partial}{\partial \boldsymbol{q}}\left(\frac{\partial C_3}{\partial \boldsymbol{q}^T}\right)\right\}\dot{\boldsymbol{q}}
\end{bmatrix} \tag{20}
$$

3 GAIT MODELS

The contact state of each legs is determined by the solution of the dynamics in Eq.(20), which is shown in the previous section. This state variously changes while walking. So we have prepared 20 kinds of gait models according to the states and have realized walking by the transition of gaits state. All of the walking dynamical models include the constrain conditions as shown in Table 2.

Table 2. Possible states for humanoid's walking

State number	State variables and constraining force and torque (Lagrange Multiplier)	Constraints (referrence)
1	$\boldsymbol{q} = [q_2, q_3, \cdots, q_{17}]^T$	Nothing
2	$\boldsymbol{q} = [q_1, q_2, \cdots, q_{17}]^T$	Nothing
3	$\boldsymbol{q} = [y_0, q_2, \cdots, q_{17}]^T$	Nothing
4	$\boldsymbol{q} = [y_0, q_1, \cdots, q_{17}]^T$	Nothing
5	$\boldsymbol{q} = [q_2, q_3, \cdots, q_{17}]^T, f_{nz}$	$C_{hz} = 0$
6	$\boldsymbol{q} = [q_1, q_2, \cdots, q_{17}]^T, f_{nz}$	$C_{hz} = 0$
7	$\boldsymbol{q} = [y_0, q_2, q_3, \cdots, q_{17}]^T, f_{nz}$	$C_{hz} = 0$
8	$\boldsymbol{q} = [y_0, q_1, q_2, q_3, \cdots, q_{17}]^T, f_{nz}$	$C_{hz} = 0$
9	$\boldsymbol{q} = [q_2, q_3, \cdots, q_{17}]^T, f_{nz}, f_{ny}$	$C_{hz}, C_{hy} = 0$
10	$\boldsymbol{q} = [q_1, q_2, \cdots, q_{17}]^T, f_{nz}, f_{ny}$	$C_{hz}, C_{hy} = 0$
11	$\boldsymbol{q} = [y_0, q_2, q_3, \cdots, q_{17}]^T, f_{nz}, f_{ny}$	$C_{hz}, C_{hy} = 0$
12	$\boldsymbol{q} = [y_0, q_1, q_2, q_3, \cdots, q_{17}]^T, f_{nz}, f_{ny}$	$C_{hz}, C_{hy} = 0$
13	$\boldsymbol{q} = [q_2, q_3, \cdots, q_{17}]^T, f_{nz}, \tau_n$	$C_{hz}, C_{fr} = 0$
14	$\boldsymbol{q} = [q_1, q_2, \cdots, q_{17}]^T, f_{nz}, \tau_n$	$C_{hz}, C_{fr} = 0$
15	$\boldsymbol{q} = [y_0, q_2, q_3, \cdots, q_{17}]^T, f_{nz}, \tau_n$	$C_{hz}, C_{fr} = 0$
16	$\boldsymbol{q} = [y_0, q_1, q_2, q_3, \cdots, q_{17}]^T, f_{nz}, \tau_n$	$C_{hz}, C_{fr} = 0$
17	$\boldsymbol{q} = [q_2, q_3, \cdots, q_{17}]^T, f_{ny}, f_{nz}, \tau_n$	$C_{hz}, C_{hy}, C_{fr} = 0$
18	$\boldsymbol{q} = [q_1, q_2, \cdots, q_{17}]^T, f_{ny}, f_{nz}, \tau_n$	$C_{hz}, C_{hy}, C_{fr} = 0$
19	$\boldsymbol{q} = [y_0, q_2, q_3, \cdots, q_{17}]^T, f_{ny}, f_{nz}, \tau_n$	$C_{hz}, C_{hy}, C_{fr} = 0$
20	$\boldsymbol{q} = [y_0, q_1, q_2, q_3, \cdots, q_{17}]^T, f_{nz}, f_{ny}, \tau_n$	$C_{hz}, C_{hy}, C_{fr} = 0$

4 CRITERIA FOR VALIDATION OF MODEL

4.1 Verification by Mechanical Energy

To verify proposed complex models, we confirm the mechanical energy conservation law. Because to verify the conservation of mechanical energy, the equation of motion must be correct. We make the model to fall freely with the input torque $\boldsymbol{\tau}_i = 0$ and the viscous friction $\boldsymbol{D}_i = 0$. In this case, there is no friction. So, it will has no loss of energy during free fall. During the motion the mechanical energy should be saved at the initial potential energy. To derive the mechanical energy, it is necessary to calculate all of the potential energy, rotational energy and translational energy.

4.2 Calculation of Mechanical Energy

It is necessary to calculate the height of the center of gravity of each link before the calculation of the potential energy. We use the homogeneous transformation matrix to calculate it as following equation.

$$^{W}z_{Gi} = ^{W}z_i + \frac{^{W}z_{i+1} - ^{W}z_i}{2} \tag{21}$$

Here, $^{W}z_{Gi}$ is the height of the center of gravity of i-th link which seen from the world coordinate. $^{W}z_i$ is the height of the joint which seen from the world coordinate. So, we can calculate the potential energy as following equation.

$$E_p = \sum_{i=1}^{17} m_i^{W} z_i g \tag{22}$$

Here, E_p is the potential energy of the model. m_i is the mass of each link. g is the gravitational acceleration.

Then, we can calculate the rotational energy as following equation.

$$E_r = \sum_{i=1}^{17} \frac{1}{2} {}^{W}\boldsymbol{\omega}_i^{T\,W} \boldsymbol{I}_i {}^{W}\boldsymbol{\omega}_i \tag{23}$$

Here, E_r is the rotational energy of the model. $\boldsymbol{I}_i$ is the moment of inertia of each link.

Then, we can also calculate the translational energy as following equation.

$$E_t = \sum_{i=1}^{17} \frac{1}{2} m_i {}^{W}\dot{\boldsymbol{r}}_{gi}^{T\,W} \dot{\boldsymbol{r}}_{gi} \tag{24}$$

Here, E_t is the translational energy of the model, $\boldsymbol{r}_{gi}$ is the translational velocity of the center of gravity of i-th link.

Finally, the mechanical energy can be derived as following equation.

$$E_m = E_p + E_r + E_t \tag{25}$$

5 VERIFICATION SIMULATION EXPERIMENT

5.1 Transition of Mechanical Energy

This simulation experiment uses the gait model of the state number (20) in Table 2. As shown in Fig.3, the humanoid model falls freely with the condition that without any viscous friction ($\boldsymbol{D}_i$=0) and input torque ($\boldsymbol{\tau}_{input} = 0$). The Fig.4 shows the result of the mechanical energy of this free falling motion. From this result, the total of mechanical energy is kept to be constant. So it can be seen that the model is correct from the viewpoint of energy conservation. Other similar experiments were simulated using other models listed in Table 2 and confirmed that the mechanical energy with those constraints are constant.

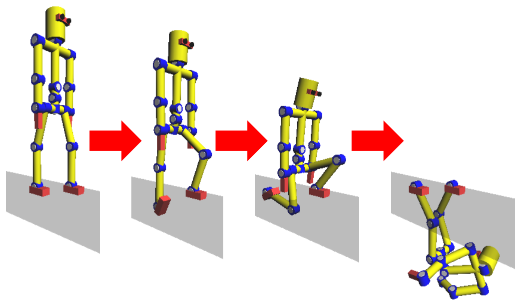

Fig. 3. Free-fall of gait model

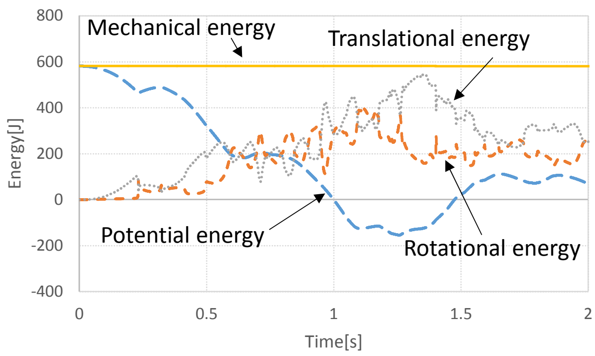

Fig. 4. In the model 20, mechanical energy confirmation experiment

5.2 Simulation Including Stick-slip

Another simulation with nonlinear friction between floor and foot are calculated to examine a stick-slip motion that can verify the humanoid model . The experiment conditions are explained as follows. The state (stick or slip) of supporting leg that is dominated by the stick-slip conditions are shown in Fig.5. When the driving force exerting to supporting leg from dynamical coupling of humanoid nonlinear model f_{y0} is larger than the maximum static frictional force f_{s0}, the supporting leg starts to slip. Here f_{n0} means the normal force exerting to the foot, and when the slip velocity of supporting leg $|\dot{y}_0|$ is less than ϵ (a very small value ϵ =0.001[m/s] $=$ 1[mm/s] in this paper), the supporting leg switches to a stick state. During the supporting leg in stick state, the coefficient of friction is set to $\mu_s = 0.8$, and when the supporting leg is in slip state, the coefficient is set to $\mu_k = 0.4$. And the body of humanoid robot falls freely without any viscous friction ($\boldsymbol{D} = \boldsymbol{0}$) and input torque ($\boldsymbol{\tau} = \boldsymbol{0}$).

$$E_{discharge} = \int_0^t \mu_k \dot{y}_0^2 dt \tag{26}$$

Figure 6 shows time profile of mechanical energy of humanoid's free-fall motion including the stick-slip motion, and Fig. 7 shows the discharged energy caused by friction on floor, the calculation of discharged energy is described in Eq.(26). Here, μ_k means the coefficient of friction when slipping, and when sticking the $E_{discharge}$ in Eq.(26) equals

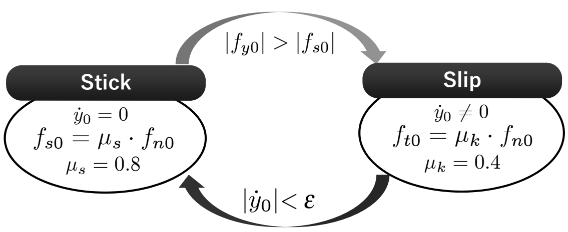

Fig. 5. Switch conditions of stick-slip motion

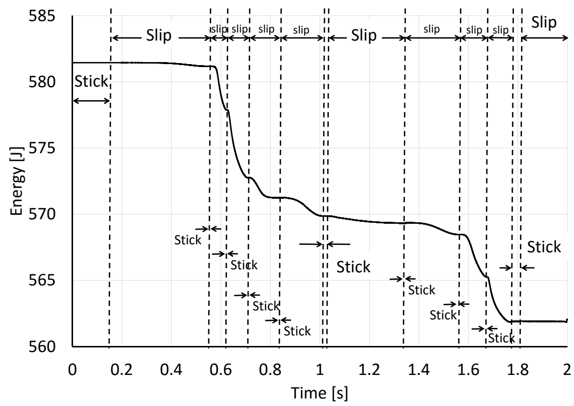

Fig. 6. Mechanical energy

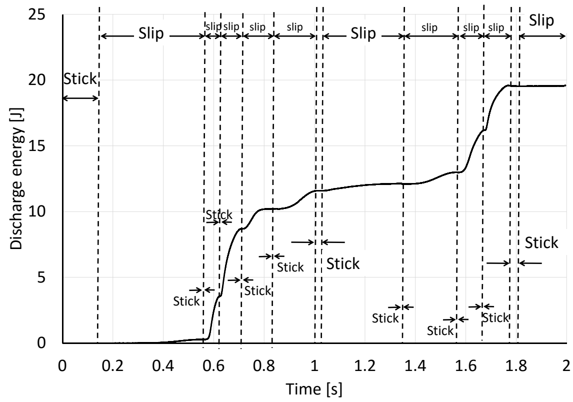

Fig. 7. Discharge of energy by friction

to zero since $\dot{y}_0$ is zero. In Figs.6 and 7, when the supporting leg is in the state of stick, the total of mechanical energy is kept at constant. And the mechanical energy discharges while the the supporting leg is slipping, and the value of discharged energy in Fig.7 is consistent with the result in Fig.6. Furthermore the velocity and the y-axis position of supporting leg are shown in Fig.8 and 9. Figure 8 shows that when the supporting leg is in the state of stick, the velocity of slip equals to zero, and Fig.9 shows that the y-axis position is also not changed in that time. And the discharge of energy depends on the velocity of slip. When the supporting leg slips fastly, when supporting leg slips faster, mechanical energy discharges larger. Conversely, when supporting leg slips very slowly or stops, the discharge of energy is also small or kept unchanged. So, from this simulation analysis, it also can be seen that supporting leg slip-stick model is consistent.

Figure 10 shows shapes of the humanoid while the simulated motion proceeds as shown from Fig.6 to 9. The configuration in Fig.10(a) was detected at the time designated by (A) in Fig.8 and Fig.9, and also (b) and (c) are the shapes at (B) and (C) in the both figures.

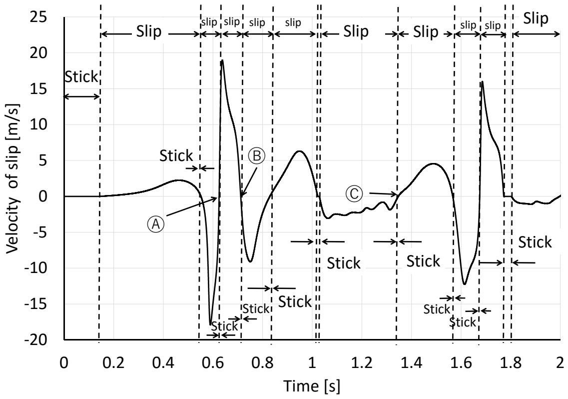

Fig. 8. Velocity of slip

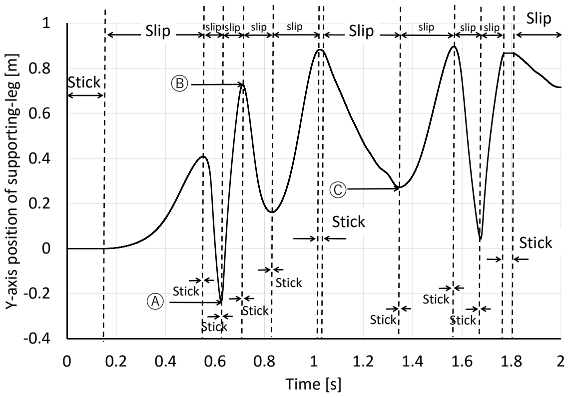

Fig. 9. y-position of supporting leg

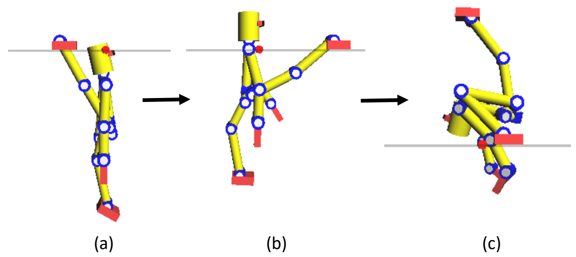

Fig. 10. Configurations during free-fall simulation shown in Fig.9, (a) the configuration at time (A) designated in Fig.9, and (b) and (c) corresponds to time (B) and (C)

6 CONCLUSION

In this paper, we showed a walking model of humanoid including slipping, bumping, surface-contacting and point-contacting of foot, which dynamical equation is derived by Newton-Euler method with constraint condition and verify the model. For the future, we plan to realize walking used slip like a ice skating.

REFERENCES

[1] S. Kajita, M. Morisawa, K, Miura, S. Nakaoka, K. Harada, K. Kaneko, F. Kanehiro and K. Yokoi, "Biped Walking Stabilization Based on Linear Inverted Pendulum Tracking," *Proceedings of IEEE/RSJ International Conference on Intelligent Robots and Systems*, pp.4489–4496, 2010.

[2] H. Dau, C. Chew and A. Poo, "Proposal of Augmented Linear Inverted Pendulum Model for Bipedal Gait Planning," *Proceedings of IEEE/RSJ International Conference on Intelligent Robots and Systems*, pp.172–177, 2010.

[3] J.H. Park and K.D. Kim, "Biped walking robot using gravity-compensated inverted pendulum mode and computed torque control," *Proceedings of IEEE International Conference on Robotics and Automation*, Vol.4, pp.3528–3593, 1998.

[4] P.B. Wieber, "Trajectory free linear model predictive control for stable walking in the presence of strong perturbations," *Proceedings of International Conference on Humanoid Robotics*, 2006.

[5] P.B. Wieber, "Viability and predictive control for safe locomotion," *Proceedings of IEEE/RSJ International Conference on Intelligent Robots and Systems*, 2008.

[6] A. Herdt, N. Perrin and P.B. Wieber, "Walking without thinking about it," *Proceedings of IEEE/RSJ International Conference on Intelligent Robots and Systems*, pp.190–195, 2010.

[7] Y. Huang, B. Chen, Q. Wang, K. Wei and L. Wang, "Energetic efficiency and stability of dynamic bipedal walking gaits with different step lengths," *Proceedings of IEEE/RSJ International Conference on Intelligent Robots and Systems*, pp.4077–4082, 2010.

[8] M. Sobotka and M. Buss, "A Hybrid Mechatronic Tiliting Robot: Modeling, Trajectories, and Control," *Proceedings of the 16th IFAC World Congress*, 2005.

[9] T. Wu, T. Yeh and B. Hsu, "Trajectory Planning of a One-Legged Robot Performing Stable Hop," *Proceedings of IEEE/RSJ International Conference on Intelligent Robots and Systems*, pp.4922–4927, 2010.

[10] Y. Nakamura and K. Yamane, "Dynamics of Kinematic Chains with Discontinuous Changes of Constraints—Application to Human Figures that Move in Contact with the Environments—," *Journal of RSJ*, Vol.18, No.3, pp.435–443, 2000 (in Japanese).

[11] J.Nishiguchi, M.Minami, A.Yanou, "Iterative calculation method for constraint motion by extended Newton-Euler method and application for forward dynamics," *Transactions of the JSME*, Vol.80, No.815, 2014.

[12] T. Feng, J. Nishiguchi, X. Li, M. Minami, A. Yanou and T. Matsuno, "Dynamical Analyses of Humanoid's Walking by using Extended Newton-Euler Method", *20st International Symposium on Artificial Life and Robotics (AROB 20st)*, 2015.

[13] M. Kouchi, M. Mochimaru, H. Iwasawa and S. Mitani, "Anthropometric database for Japanese Population 1997-98," *Japanese Industrial Standards Center (AIST, MITI)*, 2000.

[14] T. Maeba, M. Minami, A. Yanou and J. Nishiguchi: "Dynamical Analyses of Humanoid's Walking by Visual Lifting Stabilization Based on Event-driven State Transition", *2012 IEEE/ASME Int. Conf. on Advanced Intelligent Mechatronics Proc.*, pp.7-14, 2012.